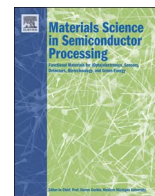




Contents lists available at ScienceDirect

## Materials Science in Semiconductor Processing

journal homepage: [www.elsevier.com/locate/mssp](http://www.elsevier.com/locate/mssp)

## Electron-optical sectioning for three-dimensional imaging of crystal defect structures

Peter D. Nellist

Department of Materials, University of Oxford, United Kingdom

## ARTICLE INFO

## Keywords:

Electron microscopy  
Defects in semiconductors  
Atomic-resolution imaging  
Three-dimensional imaging

## ABSTRACT

The depth of field of an optical imaging system is proportional to the inverse square of the numerical aperture. The development of electron-optical devices to correct for the inherent spherical aberration of electron optics has led to a dramatic increase in numerical aperture that therefore also result in dramatic reductions in depth of field. The depth of field of a state-of-the-art system may now reach below 5 nm. An opportunity is therefore created to measure three-dimensional information about a sample by focusing on specific layers within the sample, a process known as optical sectioning. In this short review, we examine some of the properties of the technique, and illustrate its use with a range of applications to semiconducting materials that have been presented in the literature.

## 1. Introduction

The development of aberration correctors in transmission electron microscopy has led to major advances in resolution and contrast both in conventional images and spectroscopic maps [1–4]. In the case of the scanning transmission electron microscope (STEM), the increased numerical aperture (NA) of the objective lens (OL) allowed by the use of aberration correctors leads to a smaller, more intense illuminating electron probe which is the origin of the improved performance. The increased numerical aperture, however, also leads to a reduction in the depth of field (DOF). Optics texts will often refer to the DOF as being inversely proportional to the square of the numerical aperture. The actual situation is somewhat more complicated and a full discussion requires consideration of the three-dimensional (3D) transfer function. Nonetheless, the DOF is very sensitive to the NA of the OL, and improvements in aberration-correction technology are leading to continual reductions in the DOF.

The reduction in DOF may be regarded as being detrimental to image interpretation if it is being assumed that the image represents a projection of the sample. In a state-of-the-art instrument the DOF may be below 5 nm – less than the typical thickness of a sample. An opportunity is created, however, to use the reduced DOF to investigate specific depths within the sample – relying on the out-of-focus regions not to strongly contribute to image contrast. This process is known as “optical sectioning”.

Here we aim to review the application of optical sectioning to the detection of defects, strain fields and the structure of dislocations and in particular dislocation cores, in semiconductor materials. Optical

sectioning can be achieved using annular dark-field (ADF) imaging in STEM, but in order to interpret the contrast, we must also consider the form of the 3D transfer function that applies. We start by highlighting some of the initial experimental results in optical sectioning, before considering how these can be interpreted in terms of the transfer function. We then go on to review the application of optical sectioning to detecting the 3D position of dopant atoms, measuring the depth-dependent strain in a sample, and the local structure of dislocations.

## 2. Initial experimental results in optical sectioning

Early applications of optical sectioning in ADF STEM came from the Pennycook group at Oak Ridge National Laboratory making use of annular dark-field STEM. A schematic of the ADF STEM experiment is shown in Fig. 1. Details of the properties of ADF STEM are described in more detail in [5], but briefly the high-angle scattering leads to an image that is strongly dependent on atomic number,  $Z$ , and the large extent of the detector leads to the image being regarded as *incoherent* which will be explained in more detail later.

Fig. 2 shows ADF STEM images from a focal series showing the gate region of a high- $k$  dielectric device presented by Van Benthem et al. [6]. Single Hf atoms in the  $\text{SiO}_2$  layer can be seen to become visible, and then disappear as the focus is changed. Using this approach the height of a number of Hf atoms could be determined. The authors noted that the Hf atoms were only visible over a range of 1.5–2.5 nm. Although the authors do not quote the beam energy and numerical aperture of their microscope, they do note that the depth of focus can be approximated to

E-mail address: [peter.nellist@materials.ox.ac.uk](mailto:peter.nellist@materials.ox.ac.uk).

<http://dx.doi.org/10.1016/j.mssp.2016.09.041>

Received 23 May 2016; Received in revised form 20 September 2016; Accepted 29 September 2016

Available online xxxx

1369-8001/© 2016 Elsevier Ltd. All rights reserved.

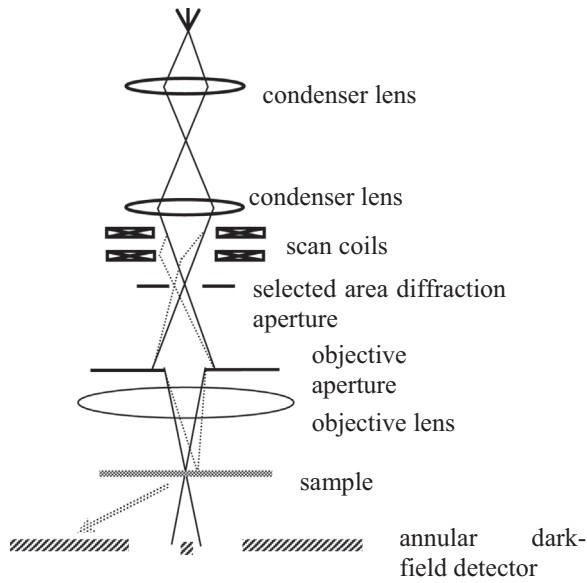


**Fig. 1.** A cross-sectional schematic of the scanning transmission electron microscope. The dashed ray paths show how the probe is scanned across the sample. High-angle scattering is detected by an annular detector as marked.

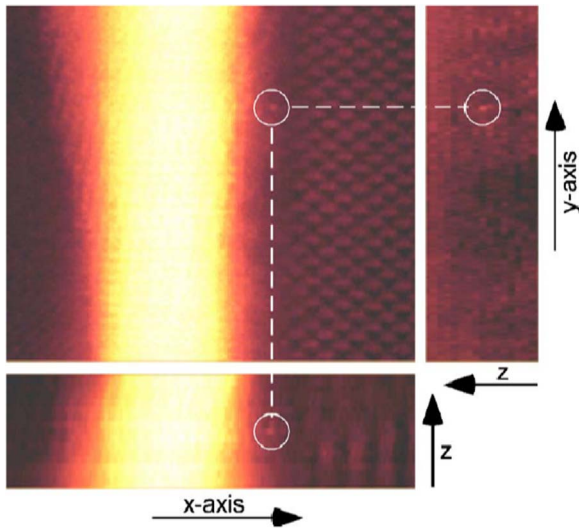


**Fig. 2.** Sections from an 3D ADF STEM image stack of a gate-oxide structure. The bright region is a  $\text{HfO}_2$  film. A single Hf atom can be seen in the amorphous  $\text{SiO}_2$  interlayer, with the Si lattice seen to the right of the image. The top left image is an  $y$ - $z$  section of the image stack at a defocus where the Hf appears. The right and bottom images show an  $y$ - $z$  and  $x$ - $z$  section from the stack at a plane containing the Hf atom. Pixel sizes are about 0.01 nm for the  $x$ - and  $y$ -directions and 0.5 nm in the  $z$ -direction, respectively. Reprinted from Ref. [6], with the permission of AIP Publishing.

$$\Delta z \sim \frac{\lambda}{\alpha^2} \quad (1)$$

where  $\lambda$  is the electron wavelength and  $\alpha$  the semi-angle of convergence of the probe-forming beam (equivalent to the NA since  $\alpha$  is small) and they mention that their depth resolution would be about 6.6 nm. They ascribe the smaller defocus variation over which the atoms were visible as arising because of the background signal and the signal-to-noise of their experiment.

This initial work was followed up with the application of optical sectioning to heterogeneous catalyst samples by Borisevic et al. [7]. The aim of the work was to detect the 3D configuration of the catalyst nanoparticles with respect to the support material. In that paper they note that the depth resolution achieved does not appear to match that given by Eq. (1). This observation was followed up more systematically

by Behan et al. [8] (Fig. 3) who found that the intensity of a nanoparticle in a 3D stack of images recorded in a focal series showed a depth profile with a full-width at half-maximum of hundreds of nanometres. They showed that for a feature of diameter,  $d$ , the integrated intensity of the scattering from that feature would only start to show a decrease once the electron probe was sufficiently defocus that it had spread wider than the feature. Mathematically this can be written as

$$\Delta z = \frac{d}{\alpha} \quad (2)$$

Assuming a nanoparticle diameter of 3.8 nm and a beam convergence semi-angle,  $\alpha$ , of 22 mrad results in an effective depth resolution of 172 nm, which corresponds well to the data shown in Refs. [8,7] and is too large to be of much use for thin TEM samples.

That the depth resolution depended on the lateral extent of the object was already known in the light-optics literature [9], but of course the much larger numerical apertures available for light optics lessens the deleterious impact of this result somewhat.

### 3. The 3D transfer function

By analogy with the light-optics literature [9], we can explore the full 3D optical transfer function (OTF) for the optical sectioning approach. The OTF is plotted in reciprocal space and is an expression of the strength of transfer to an image as a function of spatial frequency. For an object lying at a distance,  $z$ , from the focal plane of the microscope, and assuming the incoherent approximation, the image can be written as a convolution

$$I(\mathbf{R}) = P(\mathbf{R}, z) \otimes O(\mathbf{R}) \quad (3)$$

where  $P(\mathbf{R}, z)$  is the intensity of the illuminating probe as a function of lateral position,  $\mathbf{R}$ , for a microscope defocus of  $z$ , and  $O(\mathbf{R})$  is an object function that represents the scattering to the detector. Treating  $P(\mathbf{R}, z)$  as a 3D plot of the intensity in the STEM probe, the OTF can then be calculated by taking the 3D Fourier transform of  $P(\mathbf{R}, z)$ . The result, taken from [8], is shown in Fig. 4. A similar result was also shown by Intaraprasong et al. [10].

The striking feature of the OTF is the large missing cone. For spatial frequencies within this missing cone, no information will be transferred to the image. It can be seen that for low lateral spatial frequencies, the missing cone only allows low longitudinal spatial frequencies to be transferred. Thus low lateral spatial frequencies have poor depth resolution, confirming the result in Eq. (2). A confocal optical configuration can act to fill the missing cone in the transfer function, indeed this is a prime motivation for confocal microscopy. Experimental implementation of SCEM has been demonstrated [11–13]. The most effective mode in SCEM is energy-filtered SCEM, but this is hampered by the residual chromatic aberration of the optics [11]. Information outside the bounds of transfer can be reconstructed through the use of prior information, such as in a deconvolution process [14], though care must be taken over the generation of artefacts using such approaches.

If we instead focus on applications where high-lateral spatial frequencies are present, which would correspond to atomic resolution imaging, then Fig. 4 shows that high-depth resolutions can be achieved, and this is the approach used for the applications shown in the rest of this review. To summarise this section in a simple way: high-resolution images are much more sensitive to focus than lower-resolution ones, and therefore provide the highest depth resolution for optical sectioning.

### 4. Detection of individual dopant atoms and the influence of channelling

The analysis presented in Section 3 ignores the effect of scattering

Download English Version:

<https://daneshyari.com/en/article/5006055>

Download Persian Version:

<https://daneshyari.com/article/5006055>

[Daneshyari.com](https://daneshyari.com)